

Is a hyperchaotic attractor superposition of two multifractals?

K. P. Harikrishnan ^{a,*} R. Misra ^b G. Ambika ^c

^a*Department of Physics, The Cochin College, Cochin-682002, India*

^b*Inter University Centre for Astronomy and Astrophysics, Pune-411007, India*

^c*Indian Institute of Science Education and Research, Pune-411008, India*

Abstract

In the context of chaotic dynamical systems with exponential divergence of nearby trajectories in phase space, hyperchaos is defined as a state where there is divergence or stretching in at least two directions during the evolution of the system. Hence the detection and characterization of a hyperchaotic attractor is usually done using the spectrum of Lyapunov Exponents (LEs) that measure this rate of divergence along each direction. Though hyperchaos arise in different dynamical situations and find several practical applications, a proper understanding of the geometric structure of a hyperchaotic attractor still remains an unsolved problem. In this paper, we present strong numerical evidence to suggest that the geometric structure of a hyperchaotic attractor can be characterized using a multifractal spectrum with two superimposed components. In other words, apart from developing an extra positive LE, there is also a structural change as a chaotic attractor makes a transition to the hyperchaotic phase and the attractor changes from a simple multifractal to a dual multifractal, equivalent to two inter-mingled multifractals. We argue that a cross-over behavior in the scaling region for computing the correlation dimension is a manifestation of such a structure. In order to support this claim, we present an illustrative example of a synthetically generated set of points in the unit interval (a Cantor set with a variable iteration scheme) displaying dual multifractal spectrum. Our results are also used to develop a general scheme to generate both hyperchaotic as well as high dimensional chaotic attractors by coupling two low dimensional chaotic attractors and tuning a time scale parameter.

Key words:

Hyperchaotic attractor, Multifractals, Time series analysis

* Corresponding author: Address: Department of Physics, The Cochin College, Cochin-682002, India; Phone No.0484-2224954; Fax No: 91-2224954.

Email addresses: kp.hk05@gmail.com (K. P. Harikrishnan), rmisra@iucaa.in

1 Introduction

A dynamical system is considered to be chaotic if it shows the property of sensitive dependence on initial conditions. For such systems, two nearby trajectories diverge exponentially in time during the evolution of the system, indicating that one of the LEs is positive. Hyperchaos is formally defined as a state where there is divergence in at least two directions as the system evolves. Hyperchaotic attractors are thus characterized by at least two positive LEs and are considered to be much more complex in terms of topological structure and dynamics compared to low dimensional chaotic attractors. In the last two decades, hyperchaotic systems have attracted increasing attention from various scientific and engineering communities due to a large number of practical applications. These include secure communication and cryptography [1,2], synchronization studies using electro-optic devices [3,4] and as a model for chemical reaction chains [5]. In all these applications, the complexity of the underlying attractor has a major role to play.

Though the concept of hyperchaos was introduced many years ago [6], a systematic understanding of the topological and fractal structure of the attractors generated from the hyperchaotic systems is lacking till date. Studies in this direction have been very few except a series of papers on a system of unidirectionally coupled oscillators [7,8,9] in which the authors have discussed many aspects of the structure and transition to hyperchaos in the model, including dual scaling regions in the hyperchaotic phase.

Hyperchaotic attractors generated by continuous systems are, in general, higher dimensional with the fractal dimension $D_0 > 3$ and trajectories diverging in at least two directions as the system evolves in time. Hence the detection of hyperchaos is generally done using the LEs with the transition to hyperchaos marked by the crossing of the second largest LE above zero. One of our aims in this paper is to try and get a more quantitative information regarding the structure of the hyperchaotic attractor in terms of the spectra of dimensions and use this information to detect the transition to hyperchaos.

Recently, we have done a detailed dimensional analysis [10,11] of several standard hyperchaotic models and have established some results which are common to all these systems. We have applied a modified box counting scheme and have obtained an improved scaling region for computing the fractal dimension of the system. Also, we have shown that the topological structure of the underlying attractor changes suddenly as the system makes a transition from chaos to hyperchaos and there is a cross-over behavior in the scaling of the correlation dimension D_2 resulting in two different scaling regions in the hyperchaotic phase. Here we investigate this cross-over behavior in more de-

(R. Misra), *g.ambika@iiserpune.ac.in* (G. Ambika).

tail numerically and show that we can derive the whole spectrum of D_q values corresponding to the two different scaling regions. We consider this result as a consequence of the fact that the geometric structure of a hyperchaotic attractor is equivalent to that of two inter-mingled multifractals and the cross-over property is a manifestation of this structure. In other words, the overall fractal structure of a hyperchaotic attractor can be characterized by two superposed $f(\alpha)$ spectrums.

It should be noted that the *multiscales* exhibited by multifractals have recently become an interesting area of research and have been discussed in various contexts. For example, the importance of multiscale multifractal analysis (MMA) has been demonstrated in the study of human heart rate variability time series [12], where the multifractal properties of the measured signal depends on the time scale of fluctuations or the frequency band. Also, multiscale multifractal intermittent turbulence in space plasmas has been investigated in the time series of velocities of solar wind plasma [13]. In order to convince the reader that a dual multifractal structure can be realized in practice, we generate a Cantor set using variable iteration scheme which displays dual slopes in the scaling region. Finally, the specific information regarding the structure of the hyperchaotic attractor provides us the possibility of generating hyperchaos by coupling two chaotic attractors, a result already shown in the literature [14,15]. Here we present a general scheme for this to get both hyperchaos and high dimensional chaos by varying a control parameter.

Our paper is organized as follows: In the next section, we present a brief summary of the standard multifractal approach for a point set. In §3, we discuss the details of numerical computations of the multifractal spectrum to show how the structure of a hyperchaotic attractor varies from that of an ordinary chaotic attractor. In order to validate our arguments regarding the structure of the hyperchaotic attractor, we present an example of a system having analogous structure in §4 which is a synthetically generated Cantor set using a specific iterative scheme. The details regarding the generation of hyperchaos based on our numerical results are discussed in §5. The paper is concluded in §6.

2 Mathematical preliminaries

It is well known that, unlike ideal fractals, real world systems and limited point sets exhibit self similarity only over a finite range of scales [16]. Thus in the present case, statistical self similarity and hence the multifractal behavior changes between two finite range of scales. Multifractality is commonly related to a probability measure that can have different fractal dimensions on different parts of the support of this measure. Many authors have discussed the standard

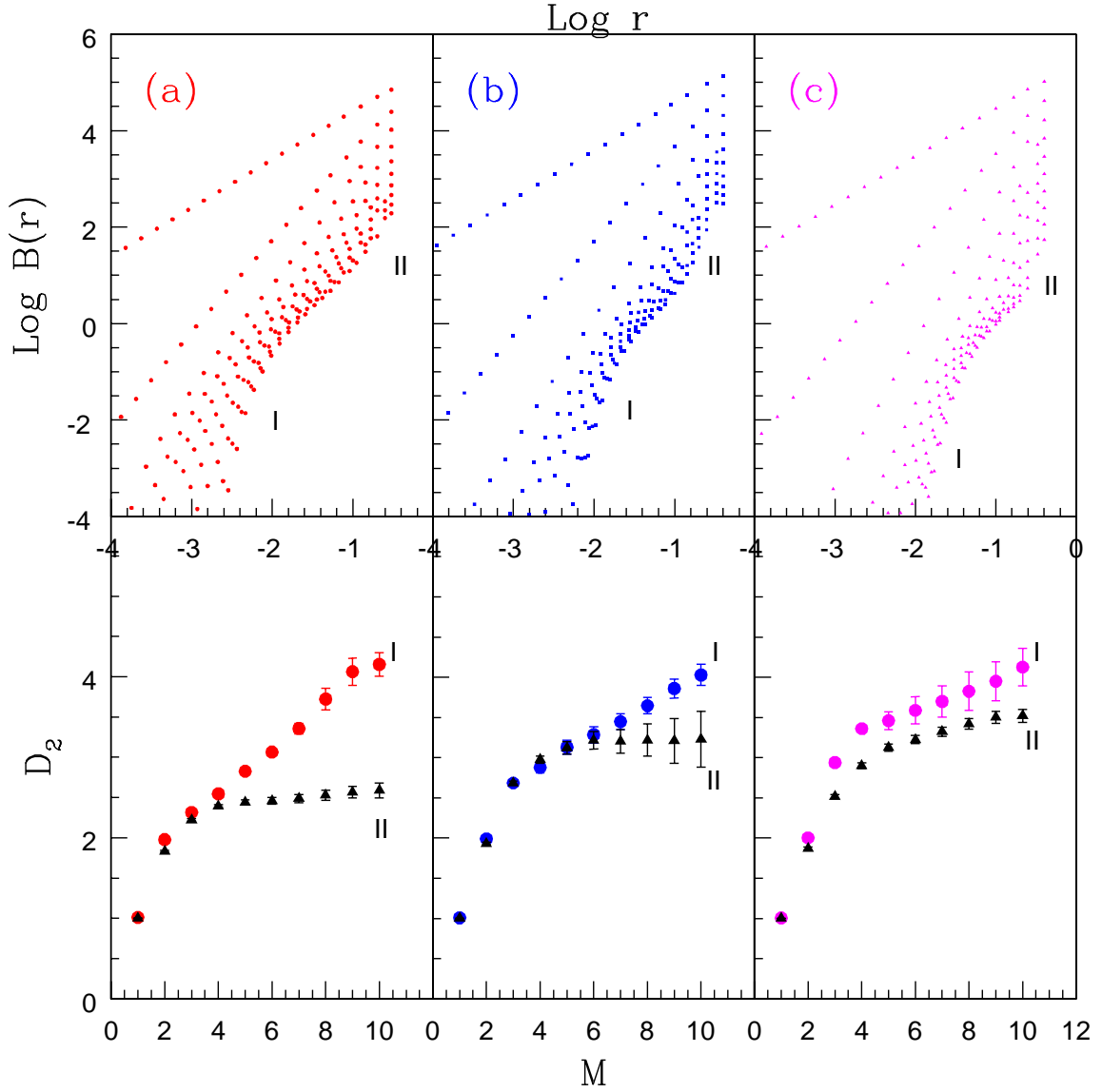


Fig. 1. Correlation dimension computed using modified box counting scheme for three different hyperchaotic time series. The top panel shows the scaling region for computing D_2 for (a) the Chen hyperchaotic flow (b) the M-G system and (c) the Ikeda system. Each curve is for an embedding dimension M that varies from 1 to 10. Two scaling regions I and II are evident in all the three cases for $M > 3$. The bottom panel shows the variation of D_2 for both scaling regions with M for the three cases.

multifractal approach in detail [17,18,19,20] and we briefly summarise the main results below for a point set (such as, an attractor generated by a chaotic system).

Let the attractor be partitioned into M dimensional cubes of side r , with $N(r)$ being the number of cubes required to cover the attractor. If $p_i(r)$ is

the probability that the trajectory passes through the i^{th} cube, then $p_i(r) = N_i/N_p$, where N_i is the number of points in the i^{th} cube and N_p the total number of points on the attractor. We now assume that $p_i(r)$ satisfies a scaling relation

$$p_i(r) \propto r^{\alpha_i} \tag{1}$$

where α_i is the scaling index for the i^{th} cube. We now ask how many cubes have the same scaling index α_i or have scaling index within α and $\alpha + d\alpha$ (if α is assumed to vary continuously). Let this number, say $g(\alpha)d\alpha$, scales with r as

$$g(\alpha) \propto r^{-f(\alpha)} \tag{2}$$

where $f(\alpha)$ is a characteristic exponent. Obviously, $f(\alpha)$ behaves as a dimension and can be interpreted as the fractal dimension for the set of points with scaling index α . This also implies that the attractor can be characterized by a spectrum of dimensions normally denoted by D_q (where q can, in principle, vary from $-\infty$ to ∞) [21], that can be related to $f(\alpha)$ through a Legendre transformation [22]. The plot of $f(\alpha)$ as a function of α gives a one hump curve with maximum corresponding to D_0 , the simple box counting dimension of the attractor.

Note that, in the above argument, the scaling exponent α measures how fast the number of points within a box decreases as r is reduced. It therefore measures *the strength of a singularity* for $r \rightarrow 0$. For a realistic attractor, with limited number of data points, the limit $r \rightarrow 0$ is not accessible and hence one chooses a suitable scaling region for r to compute α and $f(\alpha)$. This is where a hyperchaotic attractor becomes different from an ordinary chaotic attractor, as per our numerical results. We find that, to characterize the multifractal structure of a hyperchaotic attractor, two separate scaling regions are to be considered indicative of the presence of two underlying multifractals. The detailed numerical results are presented in the next section.

3 Hyperchaotic attractor as a dual multifractal

Before going into the computation of the multifractal spectrum, we discuss very briefly our results on D_2 obtained using the modified box counting scheme [10,11], where the scaling region for computing D_2 is fixed algorithmically. The attractor is covered using M -dimensional cubes of size r . The probability p_i that the trajectory passes through the i^{th} cube is computed by taking an

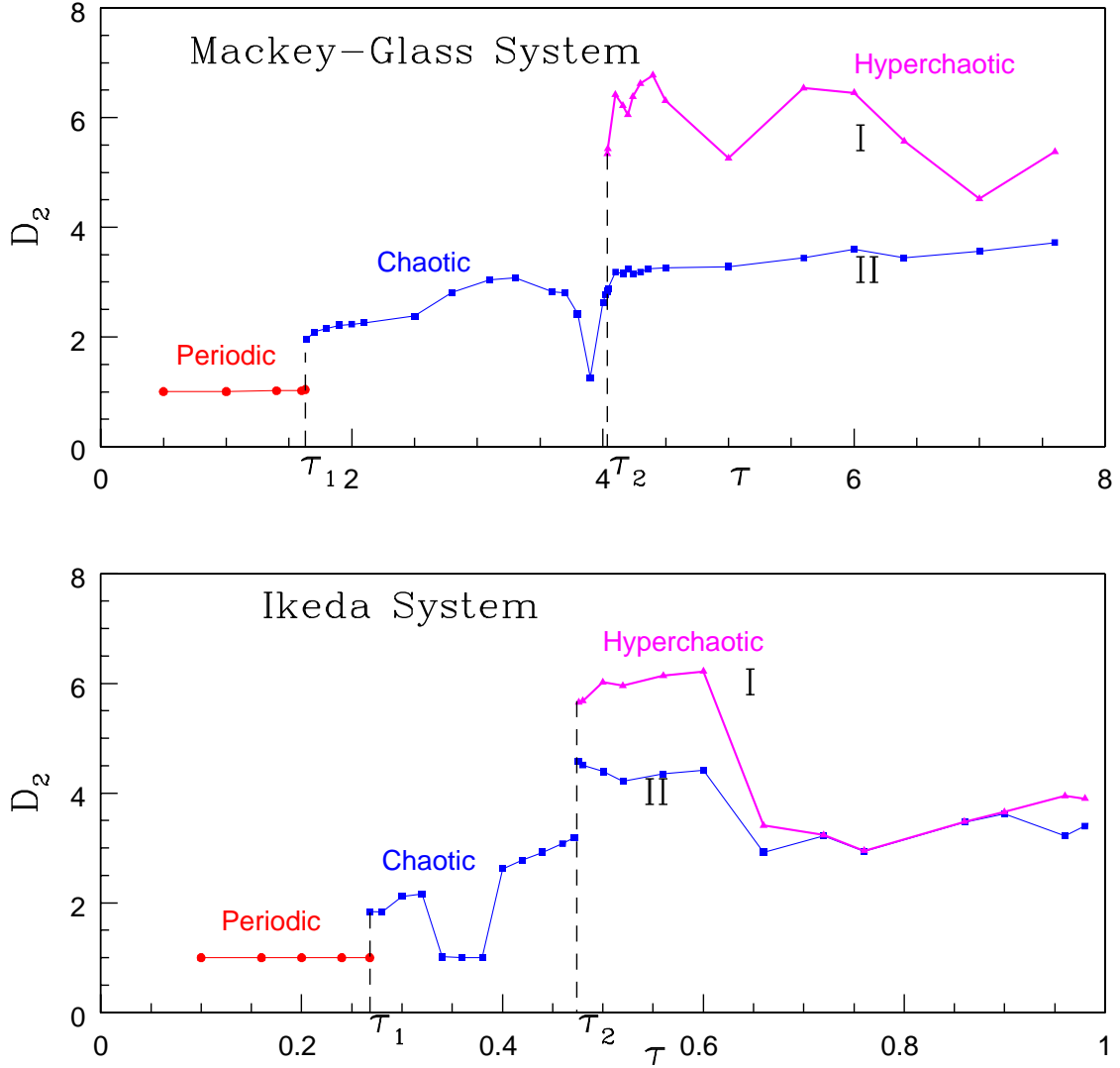


Fig. 2. Transition from periodic to chaotic and hyperchaotic phase represented as a function of the time delay parameter τ for two standard time delayed systems, with D_2 as a quantifying measure to distinguish between the three phases. Note the presence of two D_2 values in the hyperchaotic phase corresponding to two scaling regions, indicated as I and II.

ensemble average of the number of points falling in the i^{th} cube. This modifies the equation for computing the weighted box counting sum $B(r)$ as:

$$B(r) = \frac{1}{N_p^2} [\sum_i m_i^2 - N_p] \quad (3)$$

where N_p is the total number of points on the attractor and m_i is the number

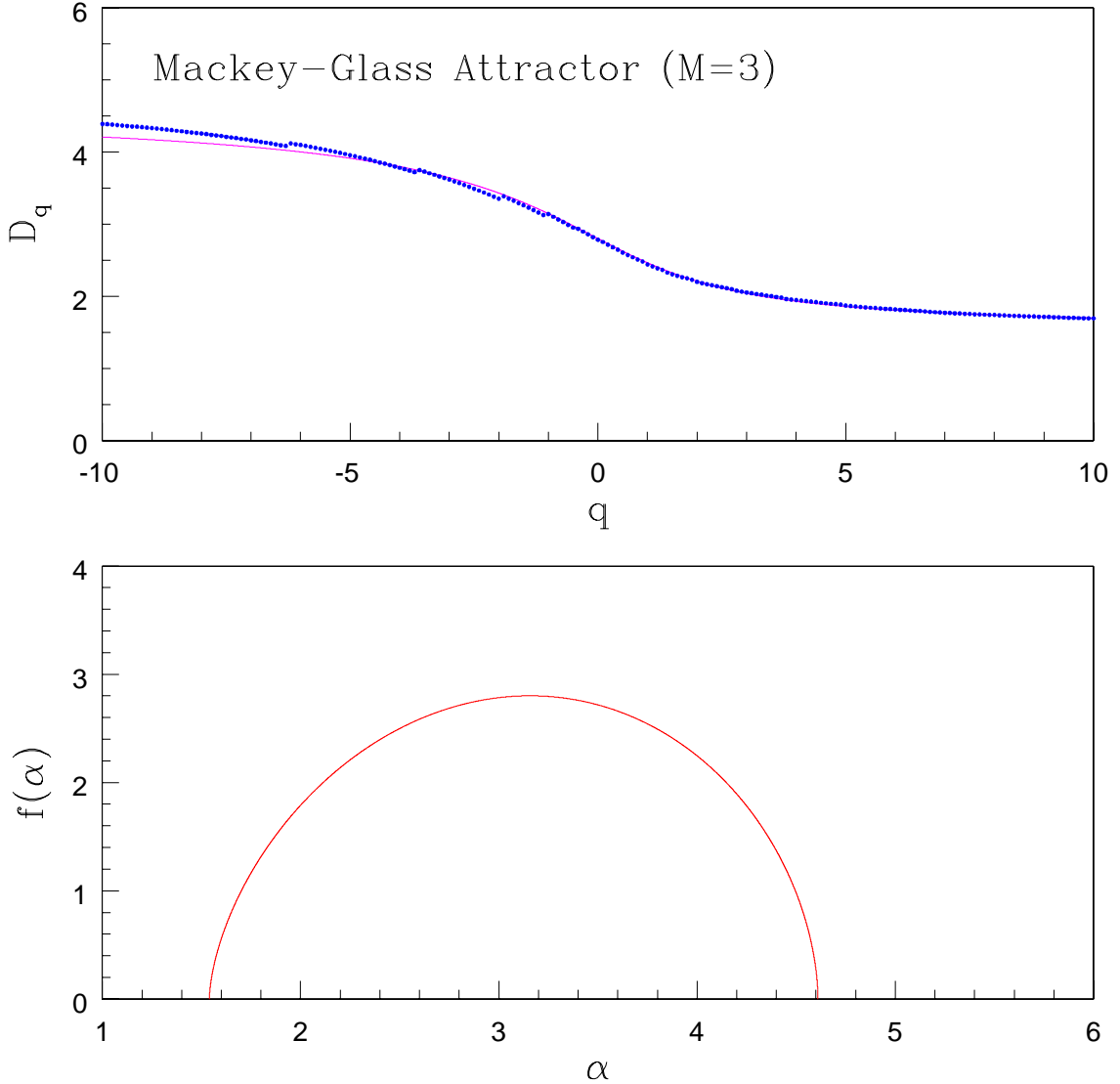


Fig. 3. Top panel shows the D_q values (points) and its best fit curve (continuous line) of the M-G attractor for $\tau = 3.70$ (in the chaotic phase), calculated from a time series consisting of 2×10^5 data points with $M = 3$. The lower panel shows the $f(\alpha)$ spectrum computed from the best fit curve.

of points falling in the i^{th} box. The correlation dimension is then calculated as the scaling index of the variation of $B(r)$ with r as:

$$D_2 \equiv \lim_{r \rightarrow 0} \log B(r) / \log(r) \quad (4)$$

For the present study, we use time series from three standard hyperchaotic systems, namely, the Chen hyperchaotic flow [23], the Mackey-Glass (M-G) time delayed system [24] and the Ikeda time delayed system [25]. For the

hyperchaotic flow, we fix the parameters as studied in detail in [10] ($a = 35, b = 4.9, c = 25, d = 5, e = 35, k = 100$) to generate the hyperchaotic time series. For M-G and Ikeda systems, we use the time delay τ as the control parameter with the other parameters fixed as $\beta = 2, \gamma = 1, n = 10$ for M-G and $a = 5, m = 20$ for Ikeda respectively. We have studied the transition to hyperchaos in these two time delayed systems in detail [11] and here we choose $\tau = 6.40$ for M-G and $\tau = 0.56$ for Ikeda for generating the hyperchaotic time series.

In Fig. 1 (top panel), we show the scaling region computed by our modified scheme for the above three systems in the hyperchaotic phase. Here, the weighted box counting sum $B(r)$ [11] is plotted against box size r . Each curve corresponds to an embedding dimension M , which varies from 1 to 10. Two scaling regions (denoted I and II) are evident in all cases, for $M \geq 4$. The D_2 values computed from the two scaling regions as a function of M are also shown in Fig. 1 (bottom panel). Based on our numerical results, the transition from chaos to hyperchaos can be identified with the sudden appearance of a second scaling region with a distinct value of D_2 . This is shown for two standard time delayed systems in Fig. 2, taking the time delay τ as the control parameter. We argue that this result is an indication of a structural change in the underlying chaotic attractor as the system makes a transition to the hyperchaotic phase at a critical value of the control parameter. The attractor changes from a simple multifractal to a dual multifractal. To convince this, we now compute the entire D_q and $f(\alpha)$ spectra corresponding to the two scaling regions separately, which is the focus of the present paper. Note that the term ‘‘dual multifractal’’ has already been used in a different context in the literature by Roux and Jenson [27] while referring to the use of two related functions to calculate the multifractal spectra by using Cantor set as example. It should not be confused with our terminology since we only use the term to indicate the structure of two inter-mingled multifractals.

To compute the $f(\alpha)$ spectrum, we use the automated algorithmic scheme proposed by us a few years back [26]. A brief discussion of the scheme is given below which is based on the Grassberger-Procaccia (G-P) algorithm [28]. As the first step, the spectrum of generalised dimensions D_q is computed from the time series using the equation

$$D_q \equiv \frac{1}{q-1} \lim_{r \rightarrow 0} \frac{\log C_q(r)}{\log r} \quad (5)$$

where $C_q(r)$ are the generalized correlation sum. This is done by choosing the scaling region algorithmically as discussed earlier [26]. We then use an entirely different algorithmic approach for the computation of the smooth profile of the $f(\alpha)$ spectrum. The $f(\alpha)$ function is a single valued function between α_{max} and α_{min} and also has to satisfy several other conditions, such as, it has

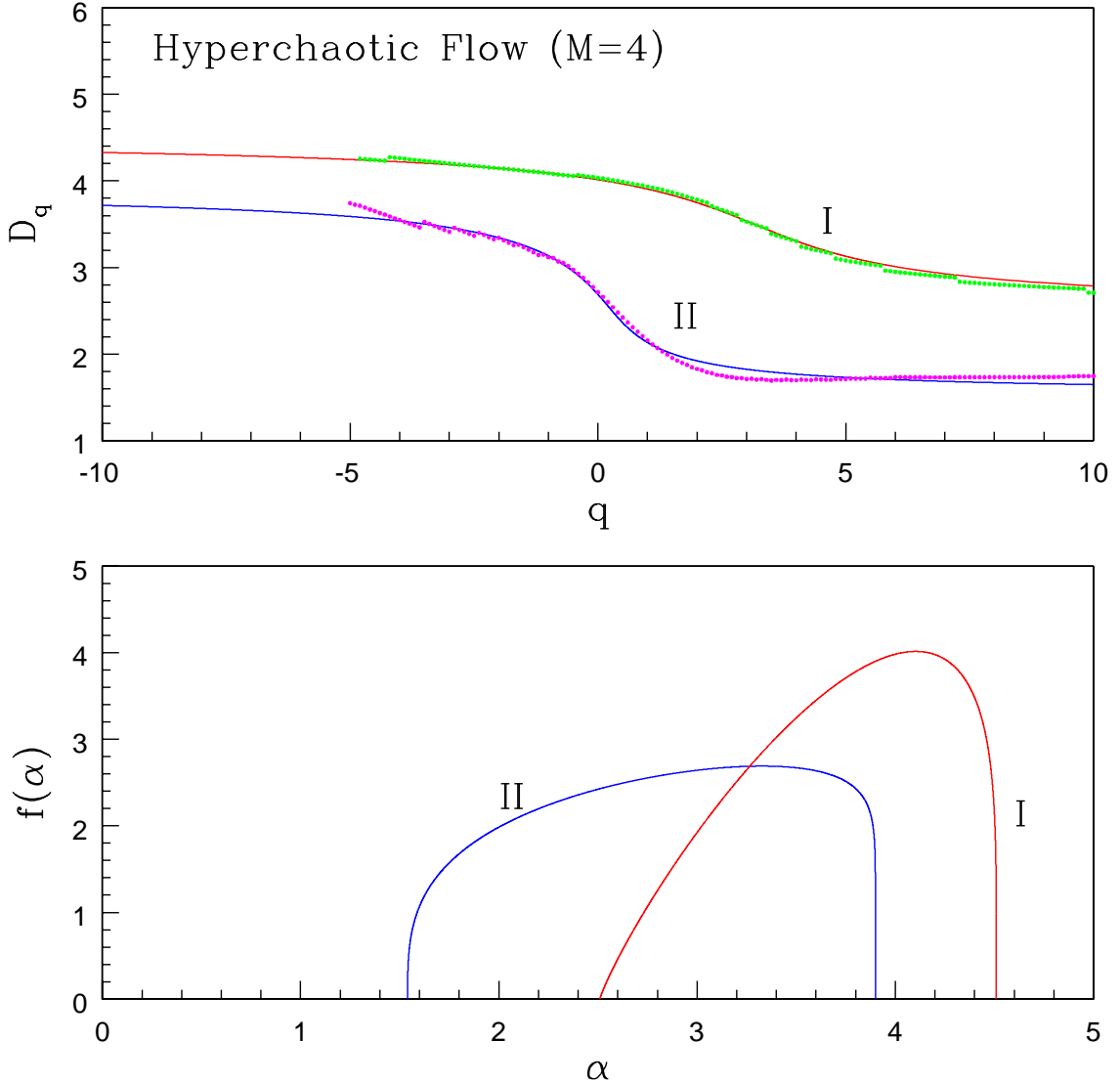


Fig. 4. Top panel shows the D_q values (points) and the best fit curve (line) for the two scaling regions of the Chen hyperchaotic flow in the hyperchaotic phase with $M = 4$. The lower panel shows the corresponding $f(\alpha)$ spectra computed from the best fit curves.

a single maximum and $f(\alpha_{max}) = f(\alpha_{min}) = 0$. A simple function that can satisfy all the necessary conditions is

$$f(\alpha) = A(\alpha - \alpha_{min})^{\gamma_1}(\alpha_{max} - \alpha)^{\gamma_2} \quad (6)$$

where A , γ_1 , γ_2 , α_{min} and α_{max} are a set of parameters characterizing a particular $f(\alpha)$ curve. It can be shown [26] that only four of these parameters are independent and any general $f(\alpha)$ curve can be fixed by four independent

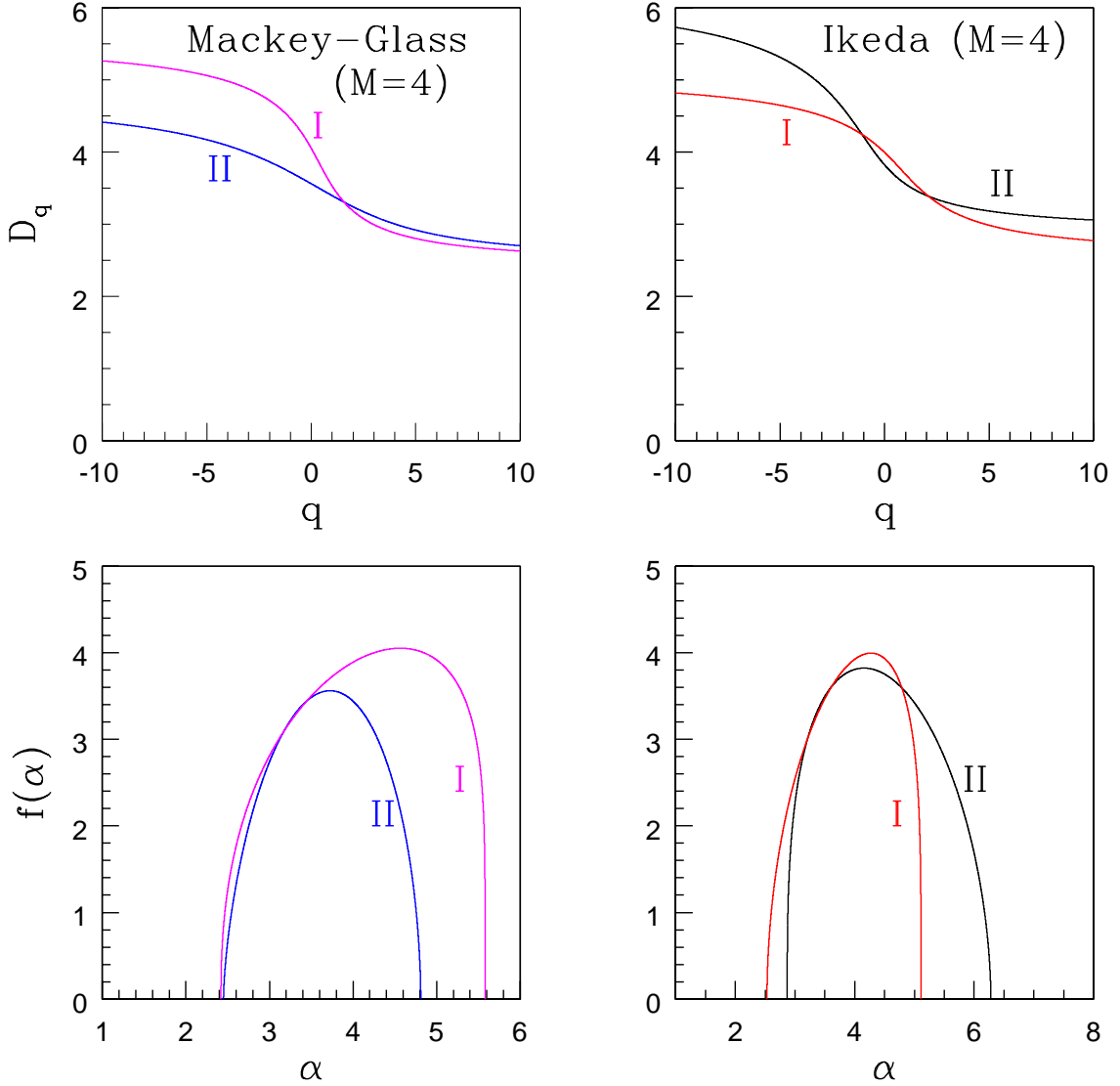


Fig. 5. The best fit D_q curves (top panel) for the two time delay systems and their corresponding $f(\alpha)$ spectra (bottom panel) in the hyperchaotic phase.

parameters. Moreover, by imposing the conditions on the $f(\alpha)$ curve, it can also be shown that $0 < \gamma_1, \gamma_2 < 1$.

The scheme first takes $\alpha_1 (\equiv D_1)$, $\alpha_{min} (\equiv D_\infty)$ and $\alpha_{max} (\equiv D_{-\infty})$ as input parameters from the computed D_q values and choosing an initial value for γ_1 in the range $[0, 1]$, the parameters γ_2 and A are calculated. The $f(\alpha)$ curve is then computed in the range $[\alpha_{min}, \alpha_{max}]$. From this, a smooth D_q versus q curve can be obtained by inverting using the Legendre transformation equations, which is then fitted to the D_q spectrum derived from the time series. The parameter values are changed continuously until the D_q curve matches with

the D_q spectrum from the time series and the statistically best fit D_q curve is chosen. From this, the final $f(\alpha)$ curve can be evaluated.

To illustrate the scheme, we first compute the D_q values and the associated $f(\alpha)$ spectrum for the M-G attractor in the chaotic phase for $\tau = 3.70$ with embedding dimension $M = 3$. The results are shown in Fig. 3. The D_q values (points) and the best fit curve (continuous line) are shown in the upper panel while the associated $f(\alpha)$ spectrum computed from the best fit curve is shown in the lower panel.

We now apply the scheme to the hyperchaotic attractors and compute the D_q and the $f(\alpha)$ spectrum for the two scaling regions separately, by fixing $r_{min}^I(r_{min}^{II})$ and $r_{max}^I(r_{max}^{II})$ for scaling region I (II). The embedding dimension used is $M = 4$ and the number of data points in the time series is 3×10^5 in all cases. Fig. 4 shows the results of computations of the Chen hyperchaotic flow while Fig. 5 shows that of the two time delayed systems in the hyperchaotic phase. In both cases, the D_q curves corresponding to the two scaling regions are given in the upper panel and the associated $f(\alpha)$ spectra are given in the lower panel. Our results indicate that the fractal structure of a hyperchaotic attractor is much more complex compared to that of an ordinary chaotic attractor having a structure equivalent to a superposition of two multifractals.

4 A Cantor set with dual multifractal structure

Here we show that it is possible to generate synthetically a set of points in the unit interval $[0, 1]$ whose geometric structure can be represented by a dual multifractal. We call this set a *2-level 2-scale Cantor set*. The construction of this Cantor set is done as follows:

For the usual Cantor set, the measure over a unit interval $[0, 1]$ is divided into two parts with probabilities p_1 and p_2 (where $p_2 = 1 - p_1$) and assigned to two fractional length scales l_1 and l_2 respectively in the first step. This process is repeated to each of the lengths l_1 and l_2 in the second step. By continuing this process n times (with $n \rightarrow \infty$), one gets the 2 - scale Cantor set which is a multifractal.

We now modify this process slightly. The above step is repeated m times where m is a finite number which is the *level I* of construction. In the *level II*, we change the probabilities p_1 and p_2 to new values p_3 and p_4 and the fractional length scales from (l_1, l_2) to (l_3, l_4) and continue the procedure for the next n steps. The resulting set is the 2 - level 2 - scale Cantor set, whose construction is shown in Fig. 6.

To implement this numerically, we use the set of parameter values: $l_1 =$

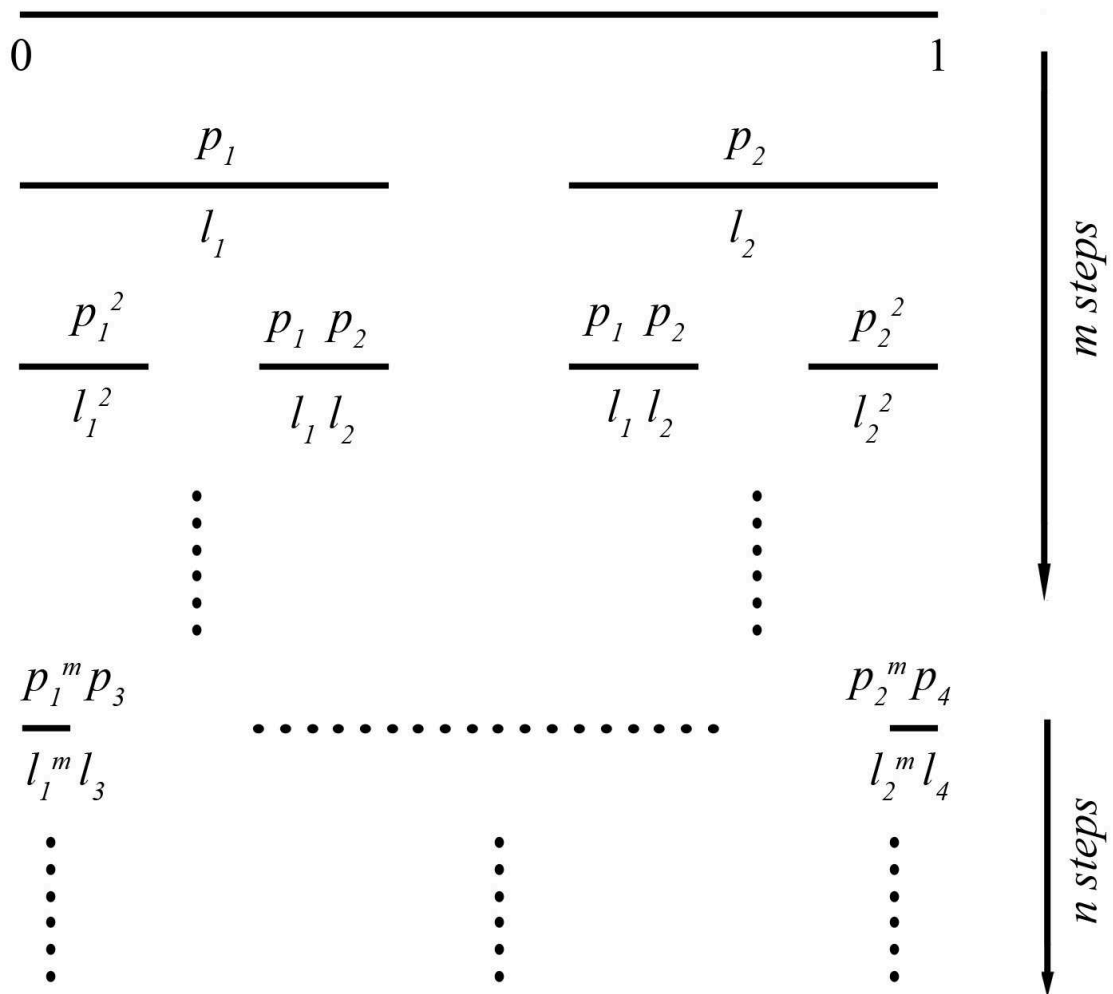


Fig. 6. Construction of 2 - level 2 - scale Cantor set. A unit interval is divided into two fractional lengths l_1 and l_2 with probabilities of measure p_1 and p_2 respectively. This process is repeated for m steps. For the next n steps, a different set of parameters (l_3, l_4, p_3, p_4) is used. The resulting set is the 2- level 2 - scale Cantor set which is a superposition of two multifractals for an intermediate range of m values.

$0.48, l_2 = 0.40, p_1 = 0.56, p_2 = 0.44, l_3 = 0.62, l_4 = 0.26, p_3 = 0.26, p_4 = 0.74$ so that the fractal dimensions of the sets generated by the two levels are widely different. We construct the set using different values of m and fixing n to be a large value (~ 5000). We find that if m is very small (say, < 20), the scaling region for the weighted box counting sum $B(r)$ as a function of r has a single slope corresponding to the fractal dimension of the Cantor set for level II and for large m (> 500), the Cantor set corresponding to level I prevails.

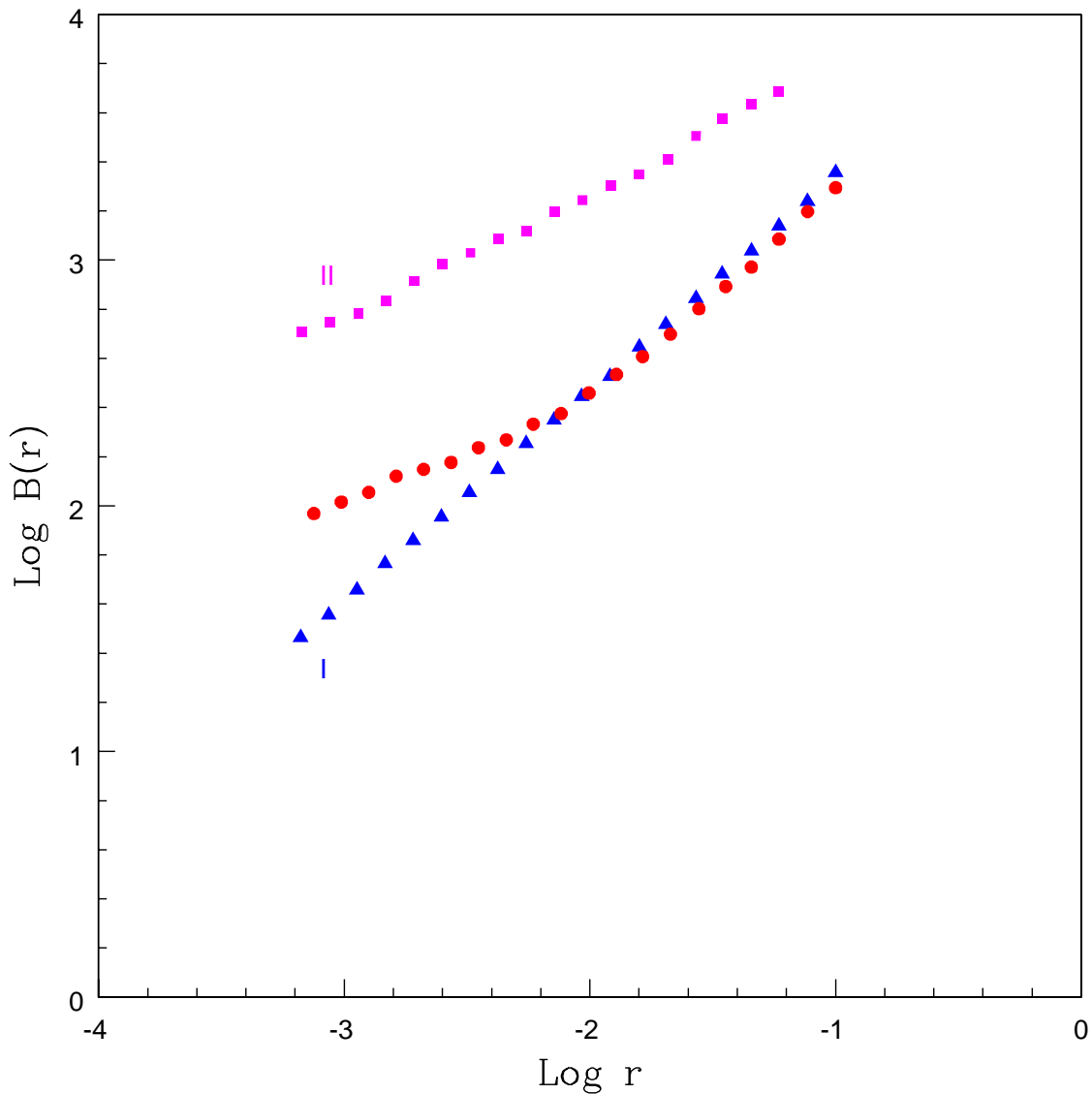


Fig. 7. Scaling region of the 2 - level 2 - scale Cantor set constructed in the previous figure. The solid triangles marked I represent the scaling region for large m corresponding to the ordinary 2 - scale Cantor set with parameters in level I while the solid squares marked II correspond to small m for the level II Cantor set. The solid circles having dual slope represent the scaling region of the resulting set for $m = 100$ which is a superposition of the two Cantor sets for levels I and II.

However, for an intermediate range of m values, the scaling region displays two slopes with a smooth transition from one to the other implying that the resulting set is a superposition of two Cantor sets involving both levels I and II. The above results are shown in Fig. 7 where the intermediate value of m used is 100. Our numerical experiment shows that the 2-level 2-scale Cantor set offers a typical geometric construction of a fractal set that displays a mul-

tifractal spectrum with two superimposed components, analogous to that of a hyperchaotic attractor which occurs in a higher dimension.

5 Generation of hyperchaos by coupling of two chaotic attractors

Finally, we show that our numerical result on the structure of a hyperchaotic attractor provides us with a possibility for constructing a hyperchaotic system by coupling two chaotic systems. There are already a few papers in the literature where the authors propose the construction of a hyperchaotic system either by coupling two chaotic systems [14,15] or by introducing a time delayed transformation [29]. It has also been suggested that in some cases, even the coupling is not required; just an amalgam of two chaotic attractors can sometimes become hyperchaotic [30,31], which strongly supports our results. This method is applied in the synchronization studies by multiplexing two chaotic signals [31]. Here we consider the prospect of generating hyperchaos by coupling any two regular chaotic systems and study under what conditions and coupling schemes one can achieve this.

The coupling of two chaotic systems is more generally employed in the synchronization studies [30] rather than hyperchaos generation where the coupling strength has to be sufficiently high. Here we consider two individual chaotic systems evolving at two different time scales coupled together. The general scheme that we propose is given by

$$\begin{aligned}\vec{X} &= \tau_{1m}\vec{F}(\vec{X}) + \epsilon_1\vec{H}(\vec{X}, \vec{Y}) \\ \vec{Y} &= \tau_{2m}\vec{F}(\vec{Y}) + \epsilon_2\vec{H}(\vec{X}, \vec{Y})\end{aligned}\tag{7}$$

Here $(\vec{X}, \vec{Y}) \in \mathcal{R}^n$ with \vec{F} representing the intrinsic dynamics of the two systems and \vec{H} denoting the coupling function. The parameters ϵ_1 and ϵ_2 represent the coupling strengths between the two systems and the parameters τ_{1m} and τ_{2m} are the two time scale parameters indicating that the two systems are evolving at two different time scales. Without loss of generality, we can take $\tau_{1m} = 1, \tau_{2m} = \tau_m$ and $\epsilon_1 = \epsilon_2 = \epsilon$.

The two individual systems \vec{X} and \vec{Y} can be any two low dimensional chaotic systems, identical or different. We have done a detailed numerical analysis taking some standard low dimensional chaotic systems, such as, Lorenz, Rössler and Ueda as individual systems with $\vec{F}(\vec{X})$ and $\vec{F}(\vec{Y})$ identical as well as different. We use the standard parameters for the individual systems in the chaotic regime. We have tried both diffusive coupling and the linear coupling, the two commonly used coupling schemes. In the former case, the feedback terms used for coupling are $\epsilon(\vec{y} - \vec{x})$ and $\epsilon(\vec{x} - \vec{y})$ while in the latter, these

are $\epsilon\vec{y}$ and $\epsilon\vec{x}$. In both cases, the 2-way or mutual coupling as well as the 1-way or drive-response coupling have been tested. The parameter ϵ should be sufficiently small (< 0.1) in order to avoid the synchronization of the dynamics between the two systems and the amplitude death [30,32]. We vary the value of ϵ in the range 0.02 to 0.05. The time step of integration Δt should be sufficiently small to capture the small scale properties of the hyperchaotic attractor and hence we fix the value of $\Delta t = 0.002$ in our numerical simulations. Our control parameter is τ_m . We have found that hyperchaos can be generated in all the different coupling schemes mentioned above for a range of values of τ_m depending on the individual systems, nature of coupling and strength of coupling.

To show the above results explicitly, we consider two specific cases. In the first case, we choose the diffusive coupling of two Lorenz systems as in drive-response mode given by

$$\begin{aligned}
\frac{dx_1}{dt} &= \sigma(x_2 - x_1) + \epsilon(y_1 - x_1) \\
\frac{dx_2}{dt} &= \gamma x_1 - x_1 x_3 - x_2 \\
\frac{dx_3}{dt} &= x_1 x_2 - \rho x_3 \\
\frac{dy_1}{dt} &= \tau_m(\sigma(y_2 - y_1)) \\
\frac{dy_2}{dt} &= \tau_m(\gamma y_1 - y_1 y_3 - y_2) \\
\frac{dy_3}{dt} &= \tau_m(y_1 y_2 - \rho y_3)
\end{aligned} \tag{8}$$

with the parameters in the chaotic regime as $\sigma = 10, \gamma = 28, \rho = 8/3$. With $\epsilon = 0.05$, the control parameter τ_m is varied and for each τ_m , 2×10^5 trajectory points are used for computing the scaling region using the modified box counting code after discarding the first 20000 points as transients.

Since we already take the time step of integration to be very small, if $\tau_m \ll 1$, the evolution of the second system turns out to be very slow and the effect of coupling will be a very small perturbation on the first system. In effect, the resulting attractor is found to be chaotic with D_2 close to that of a single system. On the other hand, when $\tau_m \gg 1$, the second system evolves very fast and often swamps out the dynamics arising out of the evolution of the first system. The result is again a chaotic attractor, but with dimension higher than the individual systems ($D_2 > 3$), resulting in high dimensional chaos. In between, for a range of values of τ_m , the resulting attractor is found to display hyperchaotic behavior. In Fig. 8, we show the results for two values of τ_m , namely, 2.4 and 20.0, the former being hyperchaotic and the latter chaotic as

reflected by the change in the scaling regions for the two cases. Note that this is analogous to what we have found in §4 in the case of Cantor set where an intermediate range of iteration steps m leads to a Cantor set with dual slopes.

The coupled Lorenz model with two different time scales as we have considered, but with two way coupling, has been used earlier as ocean-atmospheric model in climate studies [33,34] apart from synchronization studies [32]. The model represents the interactive dynamics of a fast changing atmosphere and slow fluctuating ocean. We have also analysed this model numerically with $\epsilon = 0.05$ for a range of values of τ_m . Our results indicate that the underlying dynamics can be hyperchaotic or high dimensional chaotic depending on the value of the time scale parameter τ_m .

The second case we show is a mutual diffusive coupling between the standard Lorenz and Rössler chaotic attractors given by

$$\begin{aligned}
\frac{dx_1}{dt} &= -(x_2 + x_3) + \epsilon(y_1 - x_1) \\
\frac{dx_2}{dt} &= x_1 + ax_2 \\
\frac{dx_3}{dt} &= b + x_3(x_1 - c) \\
\frac{dy_1}{dt} &= \tau_m(\sigma(y_2 - y_1)) + \epsilon(y_1 - x_1) \\
\frac{dy_2}{dt} &= \tau_m(\gamma y_1 - y_1 y_3 - y_2) \\
\frac{dy_3}{dt} &= \tau_m(y_1 y_2 - \rho y_3)
\end{aligned} \tag{9}$$

with $a = b = 0.2$ and $c = 7.8$. Here again we find that the resulting attractor is hyperchaotic for a range of intermediate values of τ_m and two typical cases, one hyperchaotic and the other high dimensional chaotic, are shown in Fig. 9. Thus we find that any two regular chaotic attractors can be coupled to generate hyperchaos as well as high dimensional chaos by varying the value of τ_m .

6 Discussion and Conclusion

Multifractality exhibited in multiscales has become an important tool for the analysis of complex systems. In this paper, we show numerically that the geometric structure of a hyperchaotic attractor is equivalent to that obtained by a superposition of two multifractal sets, with two distinct $f(\alpha)$ spectra superposed. This is shown explicitly by computing the $f(\alpha)$ spectra for two different class of hyperchaotic attractors. We show that the hallmark of such a

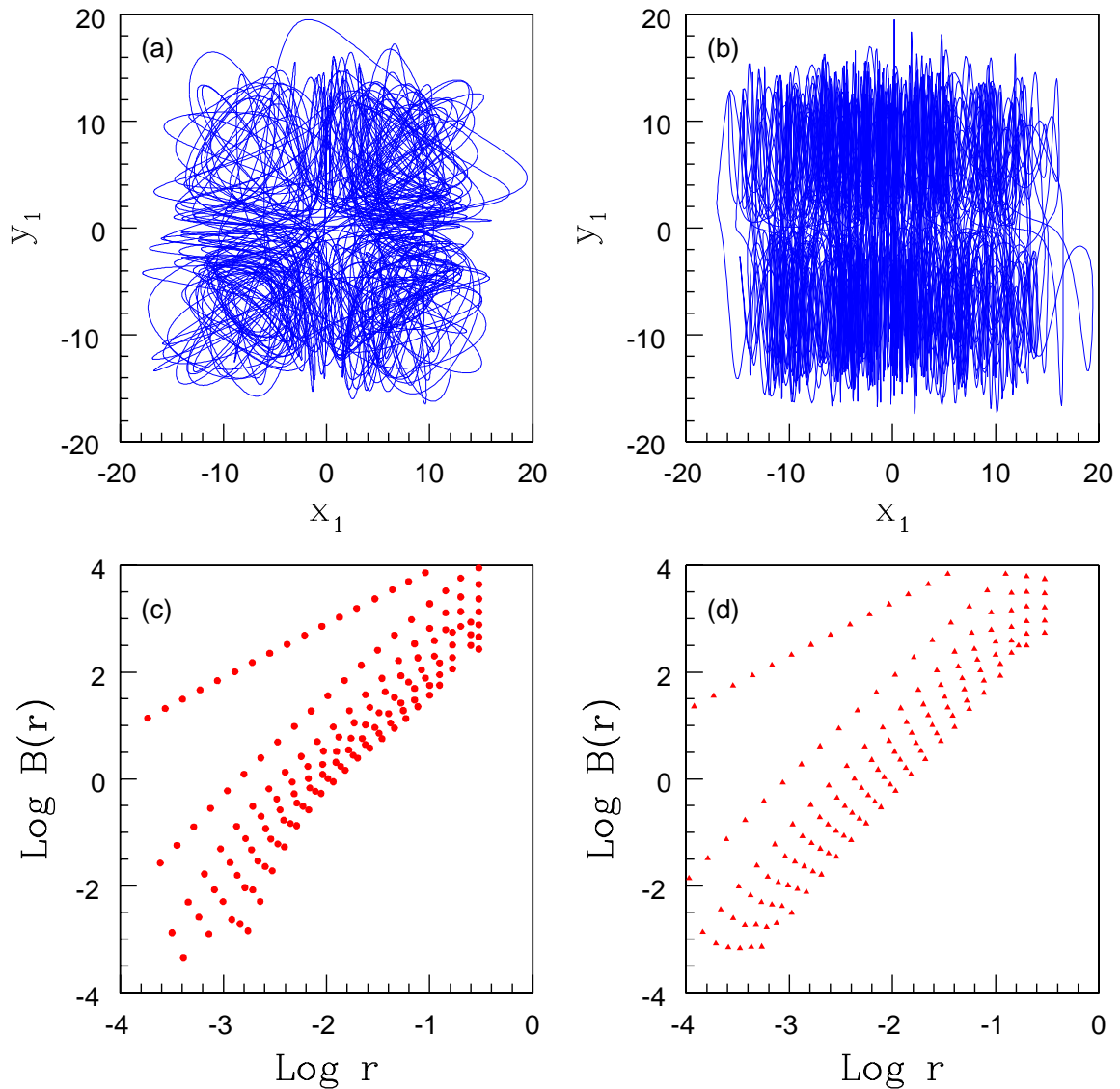


Fig. 8. Top panel shows the attractors obtained by drive-response coupling two Lorenz systems, with $\epsilon = 0.05$, as in Eq. (6) for (a) $\tau = 2.4$ and (b) $\tau = 20.0$. The corresponding scaling regions for the weighted box counting sum $B(r)$ from y_1 time series are shown in the lower panels (c) and (d) respectively. The change in the scaling region is obvious for the two τ values. While the left one is a four wing hyperchaotic attractor, the one on the right is chaotic.

structure is a cross-over behavior in the scaling region of correlation dimension. Based on our numerical results, we conjecture that a hyperchaotic attractor is a superposition of two multifractals.

Hyperchaos is normally characterized by computing the spectra of LEs and looking at the transition of the second largest LE above zero. Though this

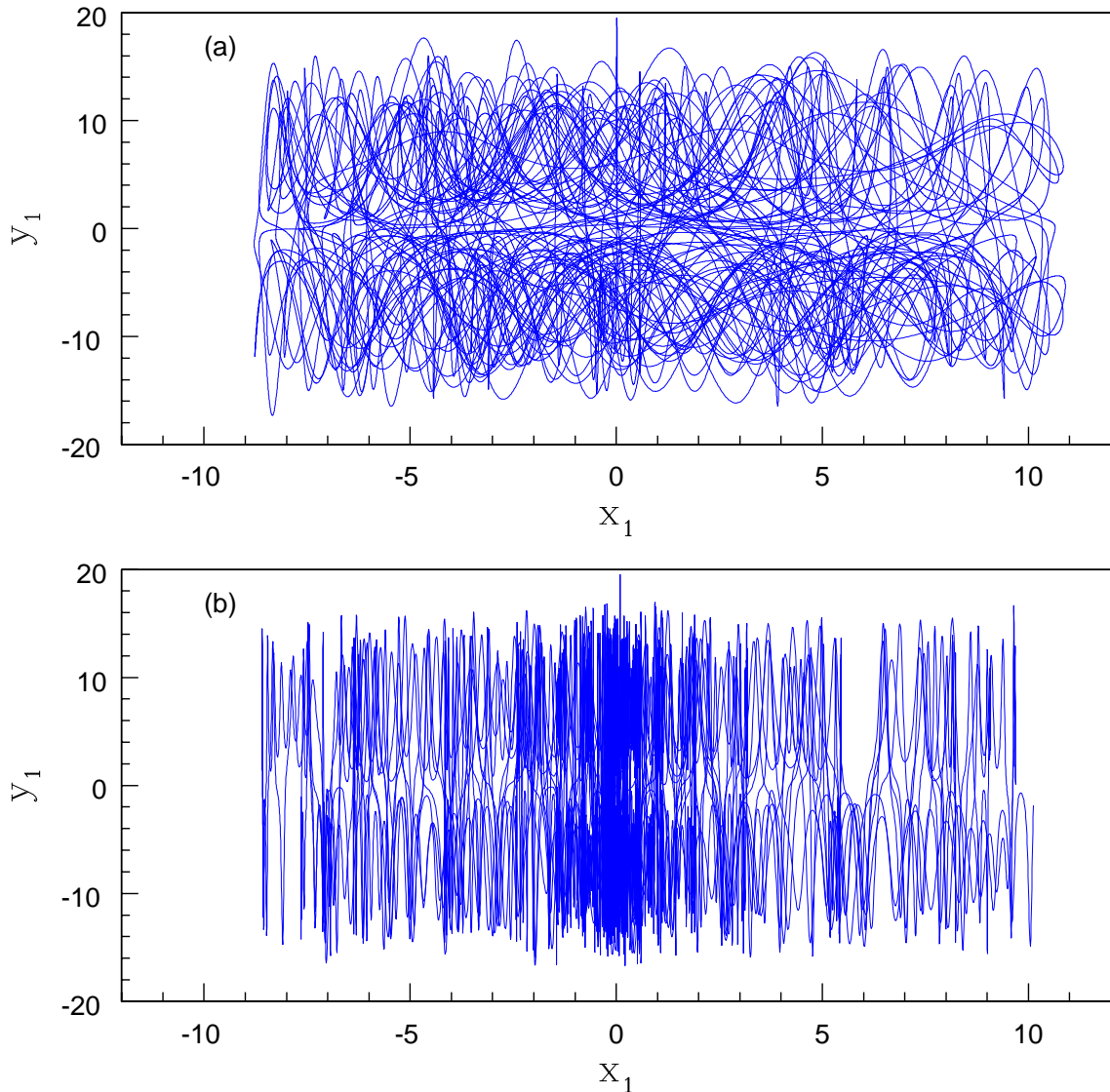


Fig. 9. Top panel is a hyperchaotic attractor arising out of the mutual diffusive coupling between the Lorenz and Rössler attractor for $\tau_m = 1.2$ and the bottom panel is a chaotic attractor for the same coupling with $\tau_m = 12.4$. In both cases, value of $\epsilon = 0.05$.

method works for synthetic systems, it becomes much more difficult when the system is represented as a time series. Our numerical results indicate that there is also a structural change for the underlying attractor as the system makes a transition to hyperchaos. This structural change can be more easily identified using the spectrum of dimensions, especially for systems analysed using time series. Thus, our results also offer a method to identify transition to hyperchaos through correlation dimension analysis of time series data. As another application, we present a general scheme by coupling two chaotic

attractors to get chaos, hyperchaos and high dimensional chaos by varying a time scale parameter.

There are two specific aspects we wish to highlight regarding the present work. We are aware that the topic of multifractality is intrinsically mathematical in nature and our claims here are based only on numerical results. A firm theoretical analysis is required to back up the results of numerical simulations presented here. We do hope that the numerical results are compelling enough to motivate a mathematical analysis in order to establish the results presented here. Secondly, we address the question how the information that hyperchaos involves a dual multifractal spectrum is important from a practical point of view. Though many authors have produced hyperchaos by coupling two low dimensional chaotic attractors, why and under what conditions this can be achieved has not been clear so far. Our results clarify both these questions and indicate that hyperchaos can be generated by suitably coupling any two low dimensional chaotic systems. Moreover, by tuning a time-scale parameter, it is possible to generate not only hyperchaos, but high dimensional chaos as well. This could be especially important in many practical applications, such as, cryptography and secure communication where the time series carrying encrypted messages needs to be novel and sufficiently complex.

Just like the dual positive LEs, a dual multifractal spectrum also appears to be characteristic of every hyperchaotic attractor as per our numerical results. However, such a structure is not unique to hyperchaotic attractors. We explicitly show an example where such a structure can be synthetically generated from a Cantor set. To our knowledge, the concept of a superposition of two multifractal sets to characterize the structure of a fractal object is novel and has not been discussed in the literature either in the context of real world fractals or those generated from dynamical systems. The results presented here clearly show that the fractal structure of a hyperchaotic attractor is qualitatively different from that of a chaotic attractor and may serve as a first step towards a better understanding of the highly complex structure of hyperchaotic attractors in high dimensional systems.

Acknowledgments

The authors thank R. E. Amritkar for the idea of generating dual multifractal from a Cantor set. KPH acknowledges the hospitality and computing facilities in IUCAA, Pune.

References

- [1] Short, K. M. & Parker, A. T., “Unmasking a hyperchaotic communication scheme” *Phys. Rev. E* **58**, (1998) 1159

- [2] Ju, J. & Cao, J., “Adaptive complete synchronization of two identical or different chaotic systems with fully unknown parameters” *CHAOS* **15**, (2005) 043901
- [3] Larger, L., Goedgebuer, J. P. & Delorme, F., “Optical encryption system using hyperchaos generated by an optoelectronic wavelength oscillator” *Phy. Rev. E* **57**, (1998) 6618
- [4] Goedgebuer, J. P., Larger, L. & Porte, H., “Optical cryptosystem based on synchronization of hyperchaos generated by a delayed feedback tunable laser diode” *Phys. Rev. Lett.* **80**, (1998) 2249
- [5] Baier, G. & Sahle, S., “Hyperchaos and chaotic hierarchy in low-dimensional chemical systems” *J. Chem. Phys.* **100**, (1994) 8907
- [6] Rössler, O. E., “An equation for hyperchaos” *Phys. Lett. A* **71**, (1979) 155
- [7] Kapitaniak, T., “Transition to hyperchaos in chaotically forced coupled oscillators” *Phys. Rev. E* **47**, (1993) R2975
- [8] Kapitaniak, T., Thylwe, K. E., Cohen, I. & Wojewodu, J., “Chaos-hyperchaos transition” *Chaos, Solitons and Fractals* **5**, (1995) 2003
- [9] Kapitaniak, T., Maistrenko, Y. & Popovych, S., “Chaos-hyperchaos transition” *Phys. Rev. E* **62**, (2000) 1972
- [10] Harikrishnan, K. P., Misra, R. & Ambika, G., “Revisiting the box counting algorithm for the correlation dimension analysis of hyperchaotic time series” *Commun. Nonlinear Sci. Numer. Simulat.* **17**, (2012) 263
- [11] Harikrishnan, K. P., Misra, R. & Ambika, G., “On the transition to hyperchaos and the structure of hyperchaotic attractors” *European Phys. J. B* **86**, (2013) 394
- [12] Gieraltowski, J., Zebrowski, J. J. & Baranowski, R., “Multiscale multifractal analysis of heart rate variability recordings with a large number of occurrences of arrhythmia” *Phys. Rev. E* **85**, (2012) 021915
- [13] Macek, W. M., Wawrzaszek, A. & Hada, T., “Multiscale multifractal intermittent turbulence in space plasmas” *J. Plasma Fusion Res. Ser.* **8**, (2009) 142
- [14] Grassi, G., Severence, F. L. & Miller, D. H., “Multi-wing hyperchaotic attractors from coupled Lorenz systems” *Chaos, Solitons and Fractals* **41**, (2009) 284
- [15] Liu, X., Shen, X. & Zhang, H., “Multi-scroll chaotic and hyperchaotic attractors generated from Chen system” *Int. J. Bif. Chaos* **22**, (2002) 1250033
- [16] Berntson, G. M. & Stole, P., “Scale limited fractals” *Proc. R. Soc. Lond. B* **264**, (1997) 1531
- [17] Hilborn, C., *Chaos and Nonlinear Dynamics*, (Oxford Univ. Press, New York, 1994)

- [18] Paladin, G. & Vulpiani, A., “Anomalous scaling laws in multifractal objects” *Phys. Reports* **156**, (1987) 147
- [19] Halsey, T. C., Jensen, M. H., Kadanoff, L. P., Procaccia, I. & Shraiman, B. I., “Fractal measures and their singularities: The characterization of strange sets” *Phys. Rev. A* **33**, (1986) 1141
- [20] Grassberger, P., Badii, R. & Politi, A., “Scaling laws for invariant measures on hyperbolic and nonhyperbolic attractors” *J. Stat. Phys.* **51**, (1988) 135
- [21] Hentschel, H. G. E. & Procaccia, I., “The infinite number of generalised dimensions of fractals and strange attractors” *Physica D* **8**, (1983) 435
- [22] Atmanspacher, H., Scheingraber, H. & Wiedenmann, G., “Determination of $f(\alpha)$ for a limited random point set” *Phys. Rev. A* **40**, (1989) 3954
- [23] Chen, Z., Yang, Y., Qi, G. & Yuan, Z., “A novel hyperchaos system only with one equilibrium” *Phys. Lett. A* **360**, (2007) 696
- [24] Mackey, M. C. & Glass, L., “Oscillation and chaos in physiological control systems” *Science* **197**, (1977) 287
- [25] Ikeda, K. & Matsumoto, K., “High dimensional chaotic behavior in systems with time-delayed feedback” *Physica D* **29**, (1987) 223
- [26] Harikrishnan, K. P., Misra, R., Ambika, G. & Amritkar, R. E., “Computing the multifractal spectrum from time series: An algorithmic approach” *CHAOS* **19**, (2009) 043129
- [27] Roux, S. & Jenson, M. H., “Dual multifractal spectra” *Phys. Rev. E* **69**, (2004) 016309
- [28] Grassberger, P. & Procaccia, I., “Measuring the strangeness of strange attractors” *Physica D* **9**, (1983) 189
- [29] Yu, P. & Xu, F., “A common phenomenon in chaotic systems linked by time delay” *Int. J. Bif. Chaos* **16**, (2006) 3727
- [30] Pecora, L. M., Carroll, T. L., Johnson, G. A., Mar, D. J. & Heagy, J. F., “Fundamentals of synchronization in chaotic systems, concepts and applications” *CHAOS* **7**, (1997) 520
- [31] Tsimring, L. S. & Sushchik, M. M., “Multiplexing chaotic signals using synchronization” *Phys. Lett. A* **213**, (1996) 155
- [32] Kajari, G. & Ambika, G., “Suppression of dynamics and frequency synchronization in coupled slow and fast dynamical systems” *European Phys. J. B* **89**, (2016) 147
- [33] Siqueira, L. & Kirtman, B., “Predictability of a low-order interactive ensemble” *Nonlinear Processes in Geophys.* **19**, (2012) 273
- [34] Soldatenko, S. & Chichkine, D., “Basic properties of slow-fast nonlinear dynamical system in the atmosphere-ocean aggregate modeling” *WSEAS Trans. on Systems* **13**, (2014) 2224